International Journal of Engineering Research
Volume No.5, Issue No.5, pp : 377-382
ISSN:2319-6890)(online),2347-5013(print)
1 May 2016

Dynamic Performance of Stand-Alone Wind-Driven Single Machine-Brushless Double Fed Generator

Maged N. F. Nashed, Mona N. Eskander, Mahmoud A. Saleh
Electronics Research Institute, Cairo, Egypt
maged@eri.sci.eg, eskander@eri.sci.eg, mahmoudsaleh36@yahoo.com

Abstract— ***In this paper the dynamic performance of a stand-alone wind-driven Single Machine-Brushless Double Fed Generator (SM-BDFIG), supplying different loads in remote area is investigated. The battery embedded in the frame of the specially designed SM-BDFIG is used for energy storage in the super synchronous range of operation. The stored energy is used to supply enough slip power for the rotor circuit of the generator in the sub-synchronous range of operation, to feed the rotor with the necessary DC power at synchronous speed, and also to supply the priority loads at low wind speeds equal or below the cut-in speed. A programmable logic controller (PLC) is designed to control the operation of the rotor converters according to the wind speed and to manage the whole stand-alone system. The dynamic performance of the generator at variable wind speeds is studied. The effect of varying loads on the generator currents, voltages, and electromagnetic torque are given for variable wind speeds. Also the effect of sudden change in the wind speed on the SM-BDFIG performance is investigated. The investigation is done at synchronous speed as well as sub-synchronous and super-synchronous speeds. Results proved the stable operation of the proposed machine as generator at within the whole speed range (from sub-synchronous speed to super-synchronous) stably.***

Keywords — Single Machine Brushless Doubly-Fed Induction Generator "SM-BDFIG", 3-phase bridge rectifier, super-synchronous operation, Battery charge, and DC link.

I. Introduction

The total global wind capacity reached 432,419 MW at the end of 2015, representing cumulative growth of 17%, according to the Global Wind Energy Council (GWEC), [i].

Wind power is leading the charge in the transition away from fossil fuels. Wind is blowing away the competition on price, performance, and reliability, and there are new emerging markets open up across Africa, Asia, and Latin America, which will become the market leaders of the next decade. Wind power led new capacity additions in both Europe and the United States, and new turbine configurations have dramatically increased the areas where wind power is the competitive option.

The electromechanical energy converter (generator), the power electronic converter and its associated controller, represent a major part of the wind energy conversion systems (WECS) components.

The main trend is to use doubly fed induction generator (DFIG) in recently manufactured WECS, due to the significant reduction in the rating of the associated converter, which was proved to be not more than 10% of the DFIG rating, [ii]. The benefits of DFIG are undeniable; however, the presence of copper slip-rings and carbon brushes to transfer electrical energy to /from the rotating winding of the generator from/to the stationary electronic converter creates the need for frequent inspection and maintenance.

The need for frequent maintenance due to the presence of brushes increases sharply the operating costs of WECS especially in remote areas and offshore installations.

A new design of brushless doubly fed induction generator BDFIM was previously proposed by the authors of this paper [iii]. The new topology of this machine, named single machine-brushless doubly fed induction generator (SM-BDFIG) is composed of three main components, namely; a regular three phase wound rotor induction machine, a power electronic converter, and a pack of rechargeable Lithium-ion batteries. The converter is mounted on the outer surface of a web-reinforced hollow metallic (aluminum) or fiber glass cylinder. The battery packs are embedded in the inner part of the cylinder between the webs. The batteries are connected together partly in series and partly in parallel, ending with output terminals carrying the full dc voltage of the whole battery pack. These two terminals are electrically connected to dc terminals of back to back converter. The ac terminals of the converter are connected to the rotor winding of the induction machine. A schematic of the SM-BDFIG is shown in Fig. (1), [v].

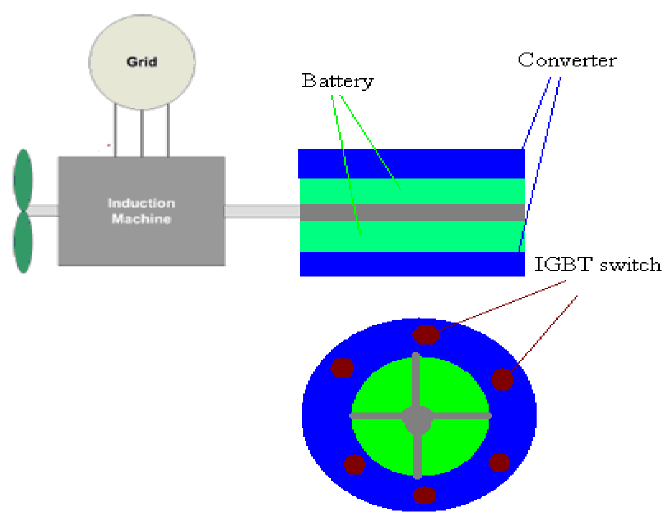

Figure (1) SM-BDFIG configuration.

In this paper the dynamic performance of the SM-BDFIG in stand-alone wind energy conversion system is fully investigated. A programmable logic controller (PLC) is employed to manage supplying the load demand. The dynamic performance of the SM-BDFIG is investigated at variable wind speeds, variable loads, and at sudden change in wind turbine speed. The investigation is performed at sub-synchronous, synchronous, and

ISSN:2319-6890)(online),2347-5013(print)
1 May 2016

super-synchronous speed. The currents, voltages, electromagnetic torque, machine speed, and battery SOC are given for these cases. Results proved the reliability and stability of the proposed system.

II. System Description

The proposed stand-alone wind generation system is composed mainly of the SM-BDFIG and PLC. A schematic of the proposed system is shown in Fig. (2)

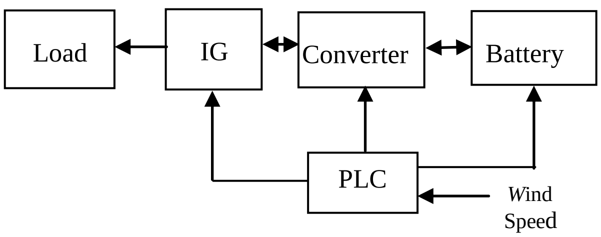

Figure (2) Block diagram of the system.

1. SM_BDFIG model

The voltage equations for the DFIG in the d-q synchronously rotating axes are given as, [vi]:

$$v_{sd} = R_s i_{sd} + \frac{d\lambda_{sd}}{dt} - \omega_s \lambda_{sq}$$
$$v_{sq} = R_s i_{sq} + \frac{d\lambda_{sq}}{dt} + \omega_s \lambda_{sd} \qquad (1)$$
$$v_{rd} = R_r i_{rd} + \frac{d\lambda_{rd}}{dt} - \omega_r \lambda_{rq}$$
$$v_{rq} = R_r i_{rq} + \frac{d\lambda_{rq}}{dt} + \omega_r \lambda_{rd}$$

Where, the stator and rotor magnetic fluxes λ are given by:

$$\lambda_{sd} = (L_{ls} + L_m) i_{sd} + L_m i_{rd}$$
$$\lambda_{sq} = (L_{ls} + L_m) i_{sq} + L_m i_{rq} \qquad (2)$$
$$\lambda_{rd} = (L_{lr} + L_m) i_{rd} + L_m i_{sd}$$
$$\lambda_{rq} = (L_{lr} + L_m) i_{rq} + L_m i_{sq}$$

where R_s, R_r, L_{ls}, and L_{lr} are resistances and leakage inductances for stator and rotor windings respectively; L_m is the mutual inductance;

v_{sd}, v_{sq},, v_{rd},, v_{rq}, are the d and q components of the stator and rotor voltages respectively

i_{sd}, i_{sq}, i_{rd}, i_{rq}, are the d and q components of the stator and rotor currents respectively

λ_{sd}, λ_{rq}, and λ_{rd}, λ_{rq} are d and q components of stator and rotor magnetic flux respectively

and ω_s and ω_r are angular frequencies of stator and rotor respectively

2. PLC Description

The Programmable logic controllers (PLCs), are computer-based solid-state devices that control industrial equipment and processes. PLCs are often the primary components in smaller control system configurations used to provide regulatory control of discrete processes such as automobile assembly lines and power plant soot blower controls. While, PLCs are control system components used throughout supervisory control and data acquisition (SCADA) or DCS systems, they can be employed to control and manage stand-alone wind energy conversion systems, [vii]

In the stand alone wind energy conversion system, proposed in this paper, the controller used for managing the system and controlling the modes of operation of the SM-BDFIG, is the PLC. It is applied to select the system configuration according to the wind speed. Figure (3) shows a schematic of the control strategy adopted using the PLC. At sub-synchronous range of operation the PLC forces the rotor converter to operate as an inverter fed from the battery incorporated in the SM-BDFIG. The inverter feeds the rotor circuit with voltage whose magnitude and frequency matches the rotor speed, i.e. varies in order to extract the maximum wind power available. The power is delivered via the machine stator. In this mode of operation the PLC switches, Q1.1 & 1.2 are opened while Q1.0 & 1.4 are closed to allow such operation.

At synchronous speed the switches are controlled to operate the SM-BDFIG as a conventional synchronous generator. i.e two phase of the rotor circuit are shorted and a DC source is applied between the shorted terminals and the third rotor terminal. In this mode of operation switches Q1.0 & 1.1 & 1.4 are opened while switch Q 1.2 is closed.

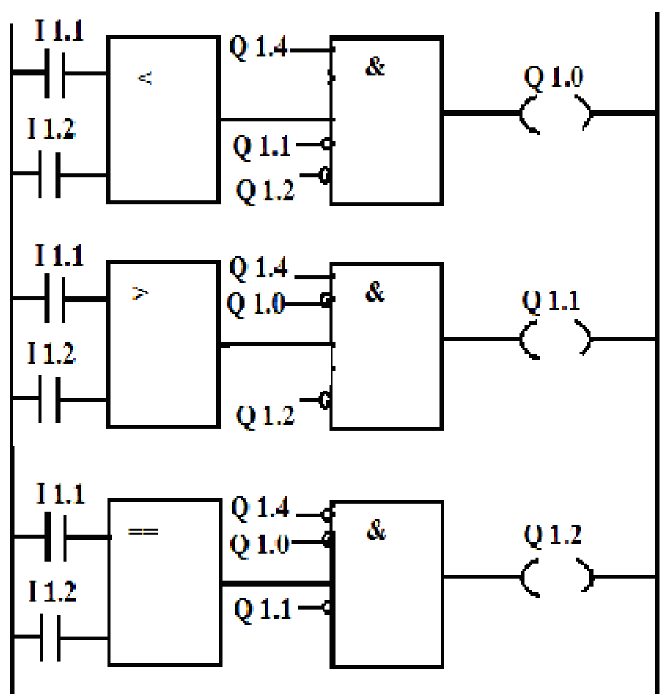

Figure (3) PLC switches.

At super-synchronous speed, the PLC allows operating the rotor converter as a rectifier used to charge the battery bank. In this

 doi : 10.17950/ijer/v5s5/508

International Journal of Engineering Research
Volume No.5, Issue No.5, pp : 377-382
ISSN:2319-6890)(online),2347-5013(print)
1 May 2016

mode of operation switches Q1.1 & 1.2, are closed while Q1.0 & 1.4 are opened to allow such operation.

Figure (4) shows the SM-BDFIG whole system including the converters and batteries controlled by PLC switches.

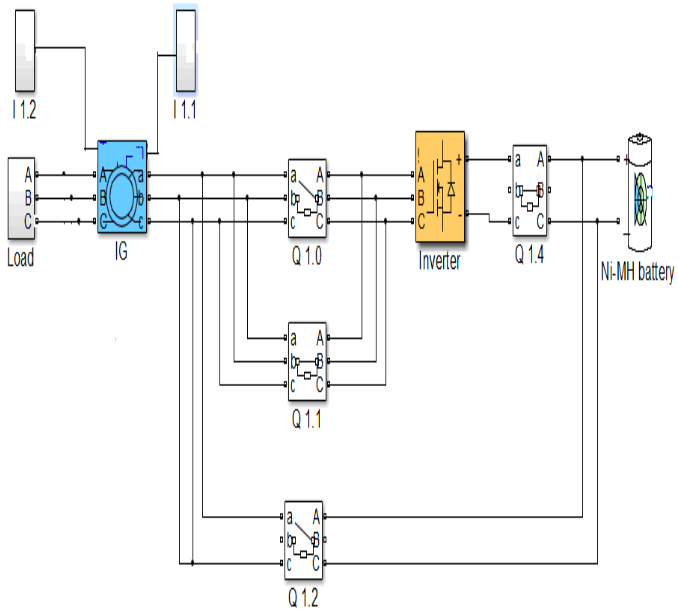

Figure (4) SM-BDFIG connections.

III. Results and Discussion due to sudden load change

The three modes of operation of the SM-BDFIG are investigated when load is changed abruptly at 0.5 sec from 150 kW to 300 kW.

1 Sub-synchronous speed

Within the sub-synchronous speed range, the battery bank applies dc voltage to converter 1, shown in Fig. (2), operated as a rectifier by the PLC. The rotor converter 2, operated as an inverter, converts the dc voltage to ac voltage at slip frequency, corresponding to the rotor speed, to feed the rotor circuit. Hence the machine operates as a generator during the sub-synchronous speed range. Figures (5) show the stator voltage, stator current, and the electromagnetic torque. Figures (6) show the rotor inverter voltage and current. Figures (7) show the load voltage, current, and power demand. Figures (8) show the battery voltage, SOC, and current, proving the ability of the batter bank to supply the rotor with the necessary voltage to operate the machine as a generator at sub-synchronous speed.

From these figures it is clear that stability is reached within small time interval, proving the reliability of the generator during dynamic operation.

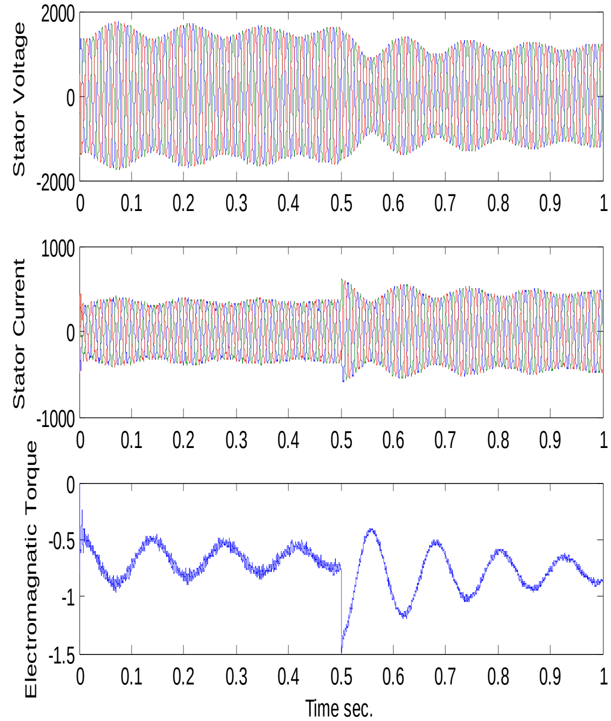

Figures (5) Stator voltages and currents, and electromagnetic torque.

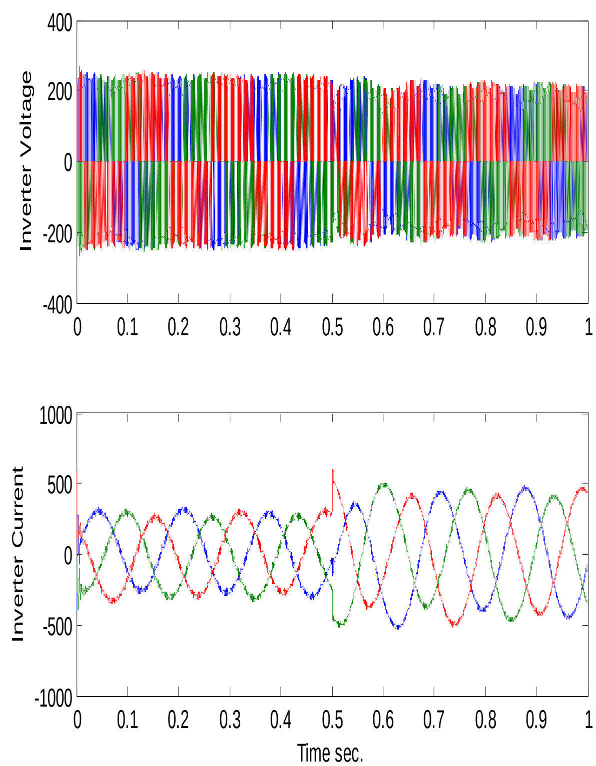

Figures (6) Rotor inverter voltage and current.

ISSN:2319-6890)(online),2347-5013(print)
1 May 2016

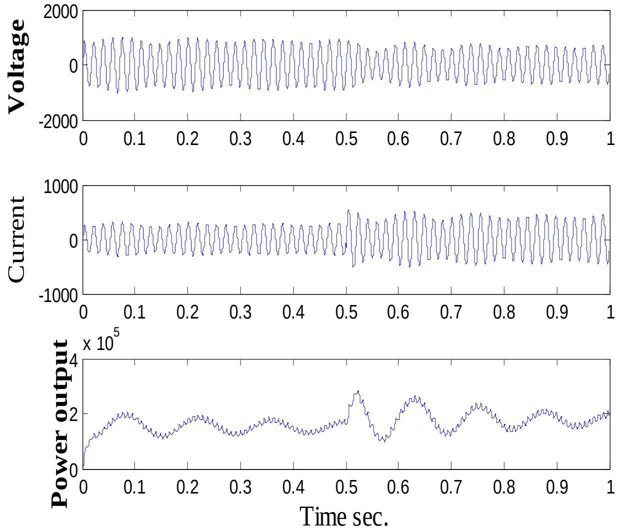

Figures (7) Voltage, current, and power output.

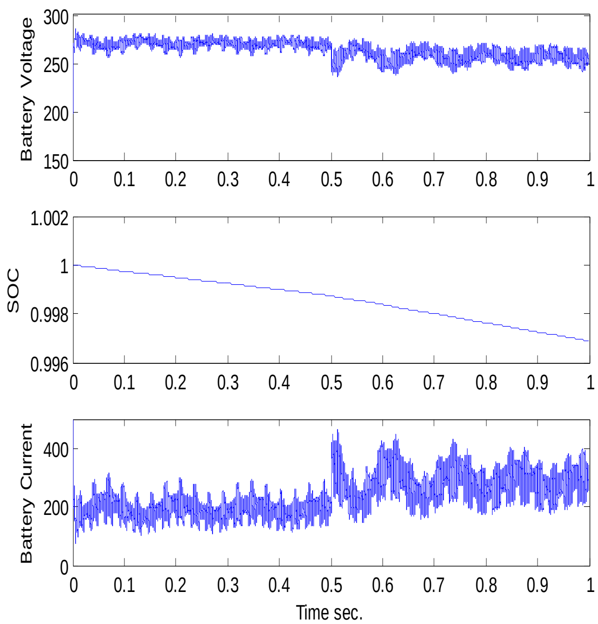

Figures (8) Battery voltage, SOC, and current.

2 Synchronous Operation

As described in section IV, the SM-BDFIG is operated as conventional synchronous generator at sub-synchronous speed. This is achieved by short-circuiting two rotor phases and connecting the common terminal to the third rotor circuit terminal via a battery. The PLC, as described, allows such operation via switches' manipulation. Figures (9) show the stator voltage, stator current, and the electromagnetic torque. Figures (10) show the load voltage, current, and power demand, proving the machine operation as a generator. However, the generated power is lower than the maximum load demand. Hence, priority loads are supplied first, using the PLC managing controller.

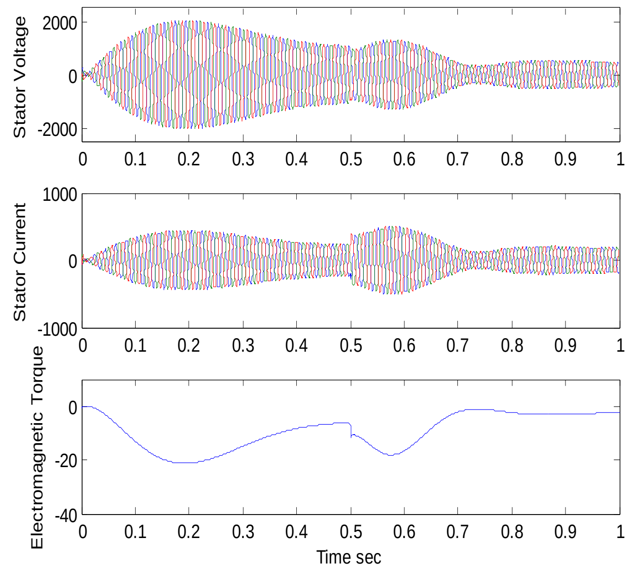

Figures (9) Stator voltage, current, and electromagnetic torque.

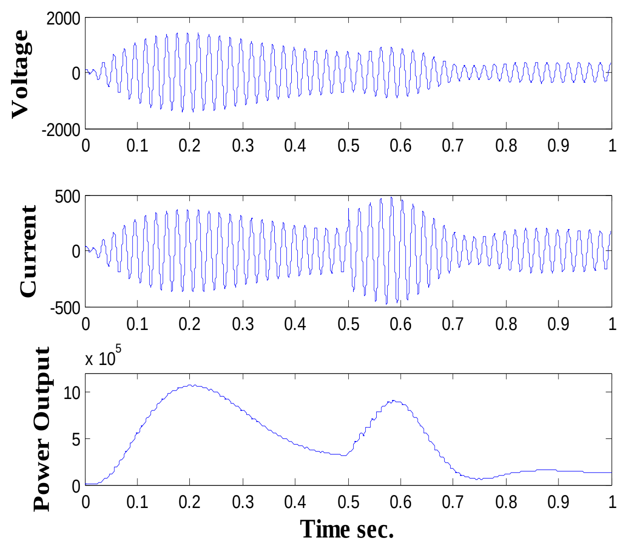

Figures (10) Voltage, current, and power output.

3. Super-Synchronous Operation

As the rotor speed increases to reach super synchronous range, the machine operates as a generator feeding the load via its stator while the rotor voltage is rectified to charge the battery. The rotor converter is operated as a rectifier to charge the battery, while the second converter is excluded. Figures (11) show the stator voltage, stator current, and the electromagnetic torque. Figures (12) show the load voltage, current, and power demand. Figures (13) show the battery voltage, SOC, and current, proving the ability of the SM-BDFIG to charge the battery bank super-synchronous speed.

The fast recovery of voltages, currents and torque prove the reliability and stability of the proposed SM-BDFIG.

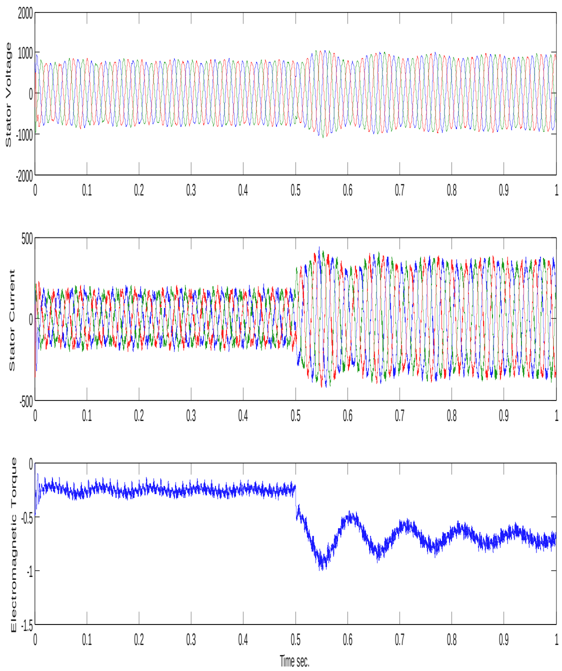

Figures (11) Stator voltage, stator current, and the electromagnetic torque.

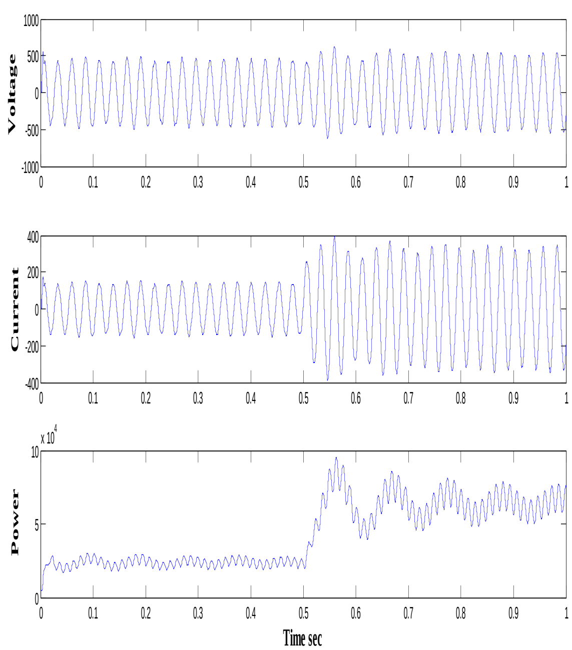

Figures (12) Voltage, current, and power output.

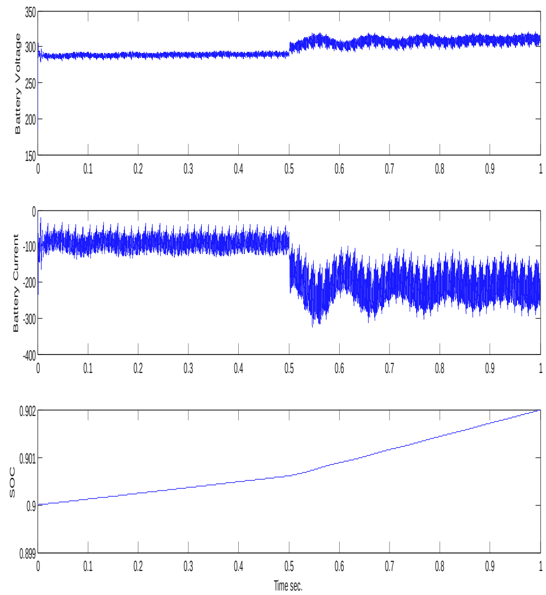

Figures (13) Battery voltage, SOC, and current.

IV. Results and Discussion due to sudden speed change

The dynamic response of the SM-BDFIG after a step change in the wind turbine speed, following wind speed variation is investigated as the speed changes from 0.998 p.u. to 1.001 p.u. at 0.4 sec. Figures (14) show the rotor voltages and current. Figure (15) stator voltage, current, Te, and speed variation. Figure (16) show the battery voltage, current, and SOC. A fast dynamic response is observed, with the machine voltages and currents acquiring the new values corresponding to the higher speed attained.

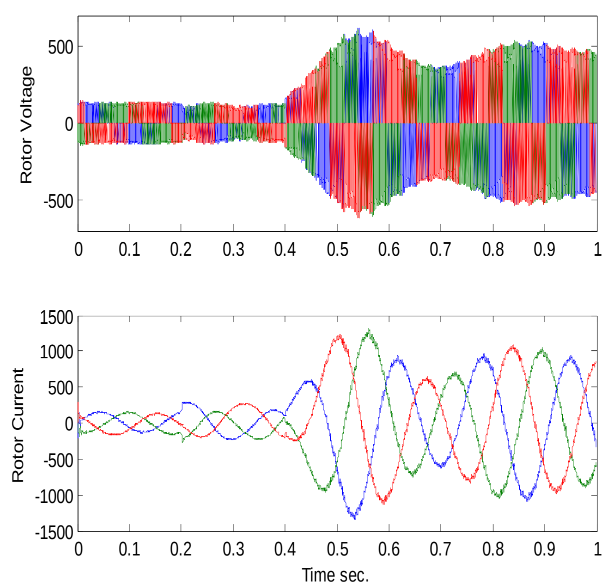

Figure (14) Rotor voltages and current.

ISSN:2319-6890)(online),2347-5013(print)
1 May 2016

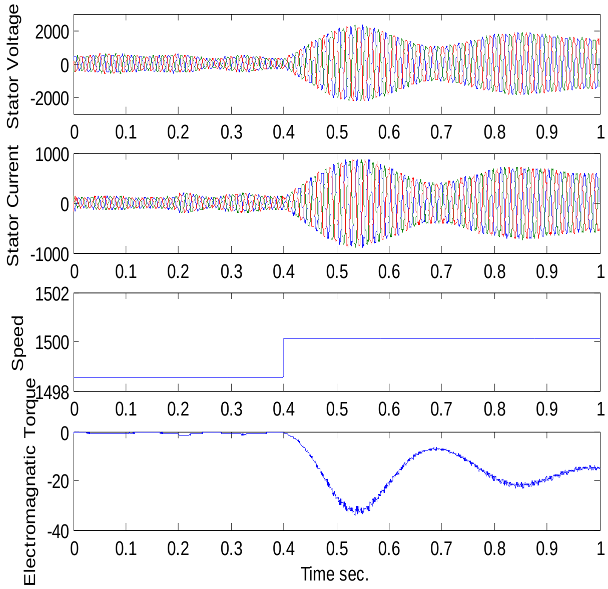

Figure (15) Stator voltage, current, and Torque.

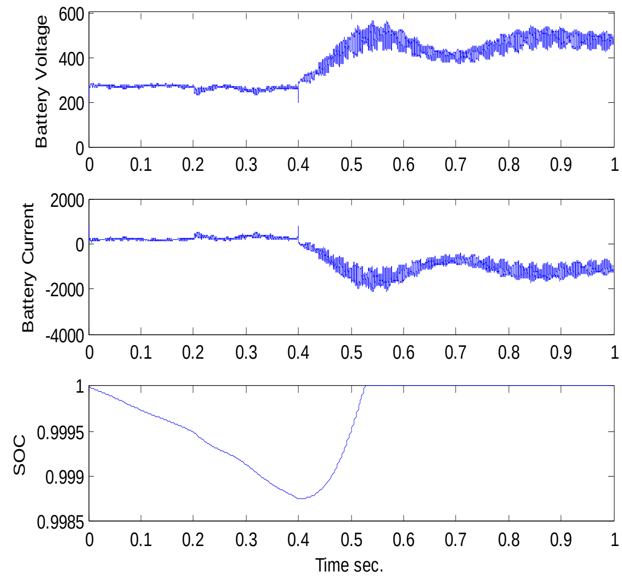

Figure (16) Battery voltage, current, and SOC.

V. Conclusion

In this paper the dynamic performance of a stand-alone wind-driven Single Machine-Brushless Double Fed Generator (SM-BDFIG), supplying variable loads in remote area is investigated. The effect of varying loads on the generator currents, voltages, and electromagnetic torque are given for variable wind speeds. Also, the effect of sudden change in the wind speed on the SM-BDFIG performance is investigated. The investigation is done at synchronous speed as well as sub-synchronous and super-synchronous speeds. Results proved the stable operation of the proposed machine as generator at within the whole speed range (from sub-synchronous speed to super-synchronous) stably, and for different load and speed conditions.

Appendix
Data of the Simulated Machine

Rated Power: 500 KVA,
Voltage : 690 Volt, 60 Hz,
No. of Poles : 4,
Stator Resistance : 10.6 m Ω,
Stator Inductance : .823 m H,
Rotor Resistance : 21.7 m Ω,
Rotor Inductance : .765 m H,
Mutual Inductance : 30.6 m H,

References

i. *Global Wind Energy Report www.gwec.net/publications/**global-wind-report**-2/*

ii. *Mahmoud A. Saleh and Mona N. Eskander, "A Single Machine Brushless DFIG for Grid-Connected and Stand-Alone WECS" British Journal of Applied Science & Technology 4 (24): 3550-3562, 2014, Sciencedomain international, www.sciencedomain.org.*

iii. *Mona N Eskander, Mahmoud Abdel Halim Saleh, and Maged N F. Nashed "Dynamic Performance of a Single Machine Brushless DFIG during Wind Speed Variation" International Journal of Engineering Research (IJER) http://www.ijer.in/ijer/ , Vol. 4, Issue No. 7, July 2015, pp: 378-383.*

iv. *Bin Zhao, Hui Li, Mingyu Wang, Yaojun Chen, Shengquan Liu, Dong Yang, Chao Yang, Yaogang Hu, and Zhe Chen, "An Optimal Reactive Power Control Strategy for a DFIG-Based Wind Farm to Damp the Sub-Synchronous Oscillation of aPower System" Energies 2014, 7, 3086-3103; doi:10.3390/en7053086, ISSN 1996-1073, www.mdpi.com/journal/energies*

v. *Mahmoud A. Saleh, Maged N. F. Nashed, and Mona N. Eskander, "An Approach to Determine the Impact of Wind Speed Variations on the Output Power of Wind-Driven DFIG", Journal of Next Generation Information Technology (ISSN: 2092-8637), Vol.3, No.1, Feb. 2012, pp7-17.*

vi. *Mahmoud Abdel Halim Saleh, Maged N F. Nashed and Mona N Eskander, "Steady State Analysis of Wind Driven SM-BDFIG in the Super-Synchronous Range of operation" International Journal of Engineering Research (IJER), **http://www.ijer.in/ijer/** Vol 4, Issue 8, August 2015, pp .412-418.*

vii. *Minkyu Choi, "Wireless Communications for SCADA Systems Utilizing Mobile Nodes", International Journal of Smart Home Vol. 7, No. 5, 2013, pp. 1-8, dx.doi.org/10.14257/ijsh.2013.7.5.01*